Hindawi Publishing Corporation
Mathematical Problems in Engineering
Volume 2015, Article ID 695962, 8 pages
http://dx.doi.org/10.1155/2015/695962

Research Article

The Heat Transfer Coefficient of Recycled Concrete Bricks Combination with EPS Insulation Board Wall

Jianhua Li[1,2] and Wanlin Cao[1]

[1]*The College of Architecture and Civil Engineering, Beijing University of Technology, Beijing 100124, China*
[2]*College of Hydraulic and Civil Engineering, Xinjiang Agricultural University, Urumqi 830052, China*

Correspondence should be addressed to Jianhua Li; ljhcwj@gmail.com

Received 31 August 2014; Revised 10 November 2014; Accepted 11 November 2014

Academic Editor: Di Zhang

Four tectonic forms samples were conducted to test their heat transfer coefficients. By analyzing and comparing the test values and theoretical values of the heat transfer coefficient, a corrected-value calculation method for determining the heat transfer coefficient was proposed; the proposed method was proved to be reasonably correct. The results indicated that the recycled concrete brick wall heat transfer coefficient is higher than that of the clay brick wall, the heat transfer coefficient of recycled concrete brick wall could be effectively reduced when combined with the EPS insulation board, and the sandwich insulation type was better than that of external thermal insulation type.

1. Introduction

As urbanization has gradually been expanding, the rapid speed of building construction and remarkable achievements in energy conservation are also expanding [1]. Energy conservation plays an important role in national energy strategies, mitigating the substantial pressure on resources and the environment [2, 3]. In building palisade components, the external wall area occupies a larger proportion, compared with the building roof, doors, windows, and so forth [4, 5]. The thermal preservation performance of the exterior wall is the key to achieving energy efficiency in buildings [5, 6]. Exterior wall differs among building materials, structural types and varies with environmental conditions. Clay brick, being widely used in many existing buildings, has caused great destruction of land resources. Its high temperature kiln firing production process has also caused the increase of greenhouse gas emissions. Therefore, a growing need of researching green wall building materials and its thermal preservation and thermal insulation performance was induced. Recycled concrete bricks, being made from crushed waste concrete, have been widely used in masonry structures as green building materials. Many studies have been carried out on its mechanical properties, but only a few measurements of its thermal insulation properties [7]. Additionally, the most common thermal insulation type was adding heat preservation materials on the outside of exterior wall, with the biggest limitation of shorter durability [8, 9]. The expandable polystyrene (EPS) used for thermal insulation played an obvious thermal preservation and thermal insulation performance. However, the diverse external wall materials with different forms of EPS heat preservation structural types, whether the variations of their thermal insulation properties are distinctly different, have not traditionally been a focus in the context of the wall heat preservation and energy conservation.

Heat transfer coefficient (U) was usually used as an index to measure the thermal preservation and insulation performance of enclosure wall and mainly decided by the thermal conductivity coefficient (λ) of the materials. Thermal and humid environment have been considered to affect the performance of enclosure wall heat transfer [10–12]. The thermal conductivity coefficient changed with air temperature and humidity, which generated to a deviation between actual value and theoretical value. However, the performance of the material parameters was assumed not to be changed

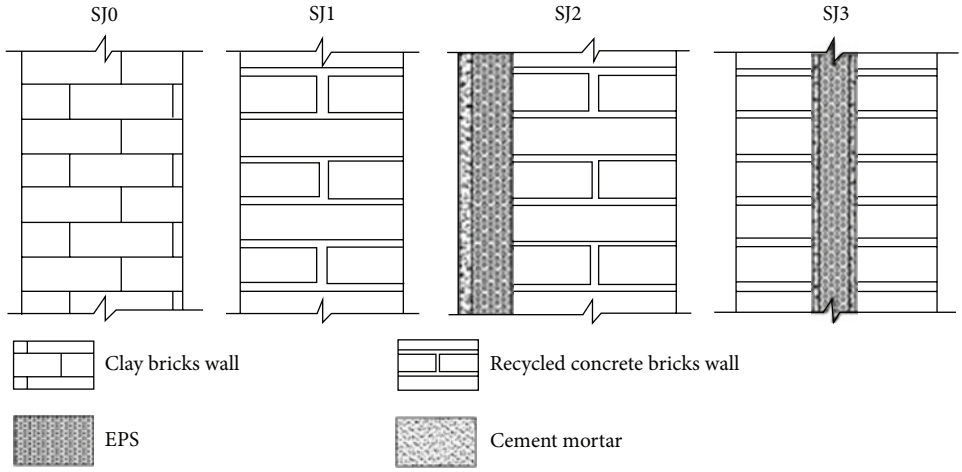

Figure 1: Tactic forms of wall samples.

Table 1: Material thickness and material properties.

Sample types	Layers	Thickness (m)	Conductivity ($W\,m^{-1}\,K^{-1}$)	Density ($kg\,m^{-3}$)
SJ0	Clay bricks wall	0.240	0.508	1662
SJ1	Recycled concrete bricks wall	0.240	0.708	1887
SJ2	1 cement mortar	0.020	0.930 [16]	1990
	2 EPS insulation board	0.060	0.042 [16]	29.50
	3 recycled concrete bricks wall	0.240	0.708	1887
SJ3	1 recycled concrete bricks wall	0.115	0.708	1887
	2 cement mortar	0.010	0.930 [16]	1990
	3 EPS insulation board	0.060	0.042 [16]	29.50
	4 cement mortar	0.010	0.930 [16]	1990
	5 recycled concrete bricks wall	0.115	0.708	1887

SJ0 was clay bricks wall; SJ1 was recycled concrete bricks wall; SJ2 was added unilateral EPS template on the basis of SJ1; SJ3 was added EPS template in the middle of SJ1.

or the coefficient of thermal conductivity (λ) of materials was expressed as a constant in many studies. Therefore, there has been growing need of studying the corrected thermal conductivity coefficient of the material in different environments and its expanded application in energy saving design.

Recycled concrete bricks have more and more potential of development and utilization. Its different combination with EPS insulation board has both the effects of green environmental protection and energy saving. Understanding the heat transfer performance of recycled concrete bricks combined with EPS insulation board becomes increasingly imperative in order to quantify their contribution to energy saving.

The objectives of this study were (1) to test heat transfer coefficient (U) of recycled concrete bricks wall, (2) to directly compare the thermal behaviors of various construction wall solutions, and (3) to put forward a corrected computational method of the heat transfer coefficient in building energy optimization.

2. Heat Transfer Coefficient Test

Currently, there is no official standard for test methods that directly address the dynamic performance of walls: the main reference norms [13] involve the measurement of steady-state characteristics of single materials and multilayer structures under standardized boundary conditions. In this study, an experimental analysis with a climatic chamber was conducted to compare the effect of heat transfer coefficient of envelope elements that are characterized by equivalent steady-state performances.

2.1. Wall Types and Material Properties. In this study, four different samples were made to quantify their thermal performances. The four samples, which were selected among the wall typologies, are detailed in Figure 1 and Table 1.

2.2. Test Apparatus. According the standards and studies concerning this type of test [14, 15], the experimental study

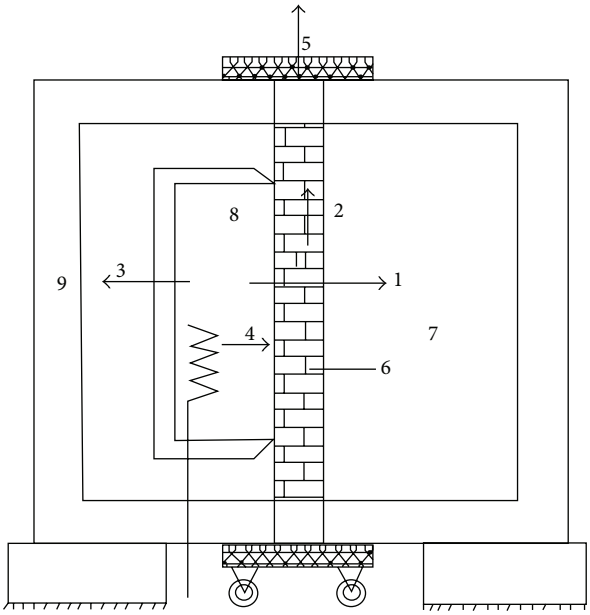

Figure 2: Environment control climate apparatus system. 1 refers to the heat flow through the samples; 2 refers to the uneven heat flow parallel to samples; 3 refers to the heat flow through the metering tank; 4 refers to the total input power; 5 refers to surrounding heat loss and the heat flow through the sample's boundaries; 6 refers to the sample; 7 refers to the cold chamber; 8 refers to the metering tank; 9 refers to the protective housing of the environment control climate apparatus.

used the steady-state heat transfer measurement apparatus (CD-WTFl515, Shenyang, China). The heat transfer condition of the tested building envelop is simulated based on the standard GB/T 13475-2008 and the single directional steady heat transfer principle to measure and analyze the heat transfer coefficient. An environment control climate facility consists of two air conditioned chambers in which temperature is controlled by heat resistance wires and refrigeration systems (Figures 2 and 3). One chamber is used to provide the outdoor environmental climate. The metering tank temperature is set to −10°C (with the permissible temperature difference of ±0.2°C). The other chamber simulates the indoor environment in which the temperature is set to 35°C (with the permissible temperature difference of ±0.1°C). The samples were made according to the stipulated size of the testing equipment. The dimensions of the facility and the samples are 2600 × 2160 × 2140 mm high and 1500 × (≤400) × 1500 mm high, respectively (Figure 4). After 28 days of natural drying in the test apparatus, the interface between the samples and test device was sealed by polyurethane foams.

All samples were tested in Beijing building materials test center. The facility was firstly calibrated before treating the wall samples in the apparatus. The indoor and outside of the wall samples must be corresponded to the hot and cold chambers, respectively. For each sample, six groups of related environment parameters data, such as temperature of the hot field (t_{ni}) and cold field (t_{ne}), humidity of the hot field (H_{ni}) and cold field (H_{ne}), and total input power (Q_p), were measured to reduce the measuring error. Nine temperature

Figure 3: The external view of the environment control climate apparatus.

Figure 4: The sample box.

sensors were connected to each side of the samples symmetrically. The permissible temperature difference of the sample surface was ±0.5°C, with a data collection interval of 10 min. The measurements were operated based on the parameters settings according to the regulation of standard GB/T 13475-2008. When the permissible temperature difference was within the value of value range after three hours continuous climate control, the tests were ended.

3. Heat Transfer Coefficient Calculation Model

The heat transfer through the wall has experienced three phases: (1) heat exchange of the inner surface; (2) thermal conductivity of internal wall; (3) heat exchange of the outside surface. Calculation methods of heat transfer in each stage are different [17], in terms of solving process of Fourier equation

with test method and the method of theory, the boundary conditions.

3.1. Test Value Calculation Principles. The test principle of steady-state heat transfer thermal performance testing apparatus (CD-WTFl515, Shenyang, China) was based on one-dimensional steady heat transfer. The samples were put between two different temperature fields to simulate the wall heat transfer in real environments. On either side of the sample, surface temperature and air temperature were measured by temperature sensors. The surface temperatures on both sides of the guide plate were also measured. Inside and outside surface temperature of metering box and input power were tested. According to the measured data that the wall heat transfer coefficient of the samples can be calculated [13], consider

$$Q_1 = M_1 \left(t_{\text{is}} - t_{\text{es}}\right), \tag{1}$$

where Q_1 is heat flow through the metering box wall (W m^{-2}), M_1 is the heat transfer coefficient of the metering wall ($\text{W m}^{-2}\,\text{K}^{-1}$), t_{is} is the internal surface temperature of the metering box (K), and t_{es} is the outside surface temperature of the metering box (K).

Then the heat transfer coefficient of the enclosure structure can be calculated according to the following formula:

$$U_0 = \left(Q_p - Q_1\right)\left[A\left(t_{\text{ni}} - t_{\text{ne}}\right)\right]^{-1}, \tag{2}$$

where Q_p is total power input (W m^{-2}), A is calculated measurement area, t_{ni} is temperature of the hot field (K), and t_{ne} is temperature of the cold field (K).

3.2. The Theoretical Calculation Model. Under the condition of steady heat transfer, when the whole process of heat transfer does not change total quantity of heat, Fourier's law can be expressed as

$$\begin{gathered} q = \left(t_i - t_e\right)\left(R_i + \sum R + R_e\right)^{-1} = \left(t_i - t_e\right) R_0^{-1}, \\ U_0 = \left(R_i + \sum R + R_e\right)^{-1} = R_0^{-1}, \\ R = d\lambda^{-1}, \end{gathered} \tag{3}$$

where q is the heat transfer of heat flow density of the structure, U_0 is the heat transfer coefficient of the building envelope ($\text{W m}^{-2}\,\text{K}^{-1}$), R_i is the heat transfer resistance of the inside surface, which is $0.11\,\text{m}^2\,\text{K W}^{-1}$, R_e is the heat transfer resistance of the outside surface, which is $0.04\,\text{m}^2\,\text{K W}^{-1}$, R is the heat transfer resistance of each material ($\text{m}^2\,\text{K W}^{-1}$), R_0 is the heat transfer resistance of the building envelope, d is the thickness of the materials (m), and λ is thermal conductivity coefficient of each material ($\text{W m}^{-1}\,\text{K}^{-1}$).

3.3. The Corrected-Value Calculation Model. The coefficient of thermal conductivity of the material is as a constant in the existing theoretical calculation and numerical calculating of the literature, without considering the material coefficient of thermal conductivity with the change of temperature and humidity. We ought to research the true value calculation of heat transfer coefficient and apply to the theoretical calculation.

3.3.1. Thermal Conductivity Coefficient Calculation under Actual Working Environment. The heat transfer mechanism of wall construction materials is similar with liquid, which is to rely on elastic waves. The thermal conductivity was increased with temperature increase and also impacted by humidity. The general equation in the case of actual working condition is usually expressed as

$$\begin{gathered} \lambda_{\text{eff}} = \lambda + \Delta\lambda_t + \Delta\lambda'_\omega + \Delta\lambda''_\omega, \\ \Delta\lambda_t = \lambda_t - \lambda, \\ \Delta\lambda'_\omega = \frac{\lambda \times 1.163\omega_v\sigma_\omega}{100}, \end{gathered} \tag{4}$$

where λ is the test value of the material thermal conductivity, $\Delta\lambda_t$ is the thermal conductivity variation aroused by temperature, $\Delta\lambda'_\omega$ is the thermal conductivity variation aroused by the weight humidity, and $\Delta\lambda''_\omega$ is the thermal conductivity variation aroused by freeze.

The λ of materials were calculated, caused by temperature difference, weight, humidity, and freeze, respectively. Then the λ of materials were calculated in work environment for the influence of thermal conductivity with temperature and humidity.

The model used to describe the effects of temperature and humidity on thermal conductivity coefficient of inorganic binding materials was [18]

$$\begin{gathered} \lambda_t = 1.163\lambda_{0^\circ\text{C}}\left(1 + 0.0025t\right), \\ \lambda_\omega = \lambda\left[1 + \left(1.163\omega_V\delta_\omega\right)100^{-1}\right], \\ \omega_V = \omega_g\rho\rho_w^{-1}, \\ \delta_\omega = 1.15\rho^2 - 6.05\rho + 14.3. \end{gathered} \tag{5}$$

The thermal conductivity tests were based on the cement mortar and recycled concrete bricks thermal conductivity testing standards [16]. The thermal conductivity variations of the materials caused by temperature, weight, humidity, and freeze then could be calculated, respectively. The thermal conductivities ($\lambda_{0^\circ\text{C}}$) (relative change for a 0°C change in t) of cement mortar and recycled concrete bricks were calculated as $0.7526\,\text{W m}^{-1}\,\text{K}^{-1}$ and $0.6160\,\text{W m}^{-1}\,\text{K}^{-1}$, respectively.

The influence of humidity on thermal conductivity coefficient of EPS template can ignore [19]. The model used to describe the effects of temperature on thermal conductivity coefficient of EPS templates was [20]

$$\lambda_t = \lambda_{10^\circ\text{C}}\left(0.9615 + 0.00399t\right), \tag{6}$$

where λ_t is thermal conductivity coefficient of inorganic binding materials at mean temperature t, λ is thermal

conductivity coefficient at 20°C, $\lambda_{0°C}$ is thermal conductivity coefficient at 0°C, t is mean temperature of the material, $\lambda_{10°C}$ is the EPS thermal conductivity coefficient at 10°C, λ_ω is moisture thermal conductivity coefficient, ω_V is the material moisture (%), δ_ω is humidity corrected coefficient, and ρ is the density of material (kg m^{-3}).

When the walls show condensation phenomenon, the daily amount of condensation can be expressed as [17]

$$\omega_g = 24\left[\left(P_A - P_{s,c}\right)H_{o,i}^{-1} - \left(P_{s,c} - P_B\right)H_{o,e}^{-1}\right], \quad (7)$$

where ω_g is the daily amount of condensation (g), P_A is the water vapor partial pressure of higher partial pressure side (Pa), P_B is the water vapor partial pressure of lower partial pressure side (Pa), $H_{o,i}$ is the water vapor permeability resistance of water vapor flowed in (m^2 h Pa g^{-1}), and $H_{o,e}$ is the water vapor permeability resistance of water vapor flowed out (m^2 h Pa g^{-1}).

3.3.2. The Corrected-Value Calculation Principles. The heat transfer of building envelope was usually calculated based on steady heat transfer, with the fixed thermal conductivities of materials being fixed values. However, the thermal conductivity, with different building envelope materials and structure types, whether the variations are distinctly different from steady heat transfer in actual work condition, has not traditionally been corrected in the context of energy saving research. Therefore, there exists a need to correct thermal conductivity on temperature and humidity. The calculation should satisfy the law of energy conservation and the heat flow density through the wall and each layer should be equal. Consider

$$\theta_m = t_i - \left(R_1 + R_2 + \cdots + R_{m-1}\right)R_0^{-1}\left(t_i - t_e\right), \quad (8)$$

where q is heat flux, q_i is wall inner surface heat flow (W m^{-2}), q_e is wall surface heat flow (W m^{-2}), q_λ is wall heat flow (W m^{-2}), θ_m is the inner surface temperature of any layer of the multilayer wall (K), t_i is indoor air temperature (K), t_e is outdoor air temperature (K), and R is heat transfer resistance (m^2 K W^{-1}).

Additionally, the calculation should satisfy that the osmotic quantity was not only proportional to the vapor pressure difference between inside and outside, but also inversely proportional to the resistance in the process of penetration. The equation is represented as

$$\begin{aligned}\omega &= \left(P_i - P_e\right)H_0^{-1}\\ P_m &= P_i - \left(H_1 + H_2 + \cdots + H_{m-1}\right)\left(P_i - P_e\right)H_0^{-1},\end{aligned} \quad (9)$$

where ω is infiltration intensity of water vapor (g m^{-2} h^{-1}), P_i is partial water vapor pressure of indoor air (Pa), P_e is partial water vapor pressure of outdoor air (Pa), H_0 is the total resistance of water vapor penetration from building envelope (m^2 h Pa g^{-1}), H is water vapor penetration resistance of materials (m^2 h Pa g^{-1}), and P_m is inner surface partial vapor pressure of any layer of the multilayer wall (Pa).

Table 2: Experimental results of the mean measured temperature of the hot field (t_{ni}) and cold field (t_{ne}), humidity of the hot field (H_{ni}) and cold field (H_{ne}), and total input power (Q_p).

Sample types	t_{ni} (°C)	t_{ne} (°C)	H_{ni} (%)	H_{ne} (%)	Q_p (W)
SJ0	34.92	−10.17	54.30	49.70	122.71
SJ1	34.91	−10.03	55.40	43.80	156.38
SJ2	34.97	−10.15	60.80	46.20	38.27
SJ3	35.09	−10.02	60.90	50.30	30.21

3.3.3. Correct Calculation of Heat Transfer Coefficient. Combined with these known values, such as the thicknesses of each wall's materials, thermal conductivities, and water vapor penetration coefficient, the temperature distribution inside the wall, the water vapor partial pressure distribution, the water content, and the amount of ice then could be calculated. This will modify the thermal conductivities of each material to calculate the heat transfer coefficient. The modified thermal conductivities were then reused to repeat the calculation. Then the heat transfer coefficient is iteratively solved until the change of values is within the convergent criterion (Figure 5).

4. Results

4.1. Experimental Results and Uncertainty Analysis. Mean values of the related environment parameters of the four samples were showed in Table 2, respectively. The uncertainty of the measurement results may be involved to several uncertainty components. The combined standard uncertainties caused by measurement repeatability (u_1) were u_1 (U_{SJ0}) = 0.23%; u_1 (U_{SJ1}) = 0.16%; u_1 (U_{SJ2}) = 0.59%; u_1 (U_{SJ3}) = 0.45%, respectively. The combined standard uncertainties caused by the power test value error (u_2) and temperature test value error (u_3) were 0.1% and 1%, in which the coverage factor (k) is 2. Therefore, the combined standard uncertainty of the heat transfer coefficient experiment was synthesized by these uncertainty components [21]. Consider

$$u_f = \left[u_1^2 + u_2^2 + u_3^2\right]^{0.5} \quad (10)$$

in which the coverage factor (k) is 2. The combined expanded uncertainties for the heat transfer coefficient were 2.06%, 2.04%, 2.33%, and 2.20%, respectively.

4.2. Test Values and Theoretical Values. Test value of heat transfer coefficient can be calculated with the wall sample test data and the calculation model (Table 3). Theoretical value of heat transfer coefficient can be calculated with theoretical calculation model. The coefficient of thermal conductivity of recycled concrete brick wall was calculated with the test results of SJ1. The heat transfer coefficients of SJ2 and SJ3 were calculated with the coefficient of thermal conductivity of recycled concrete bricks wall.

4.3. Results of Test Values and Theoretical Values. Experimental value of heat transfer coefficient of SJ0 was lower than that

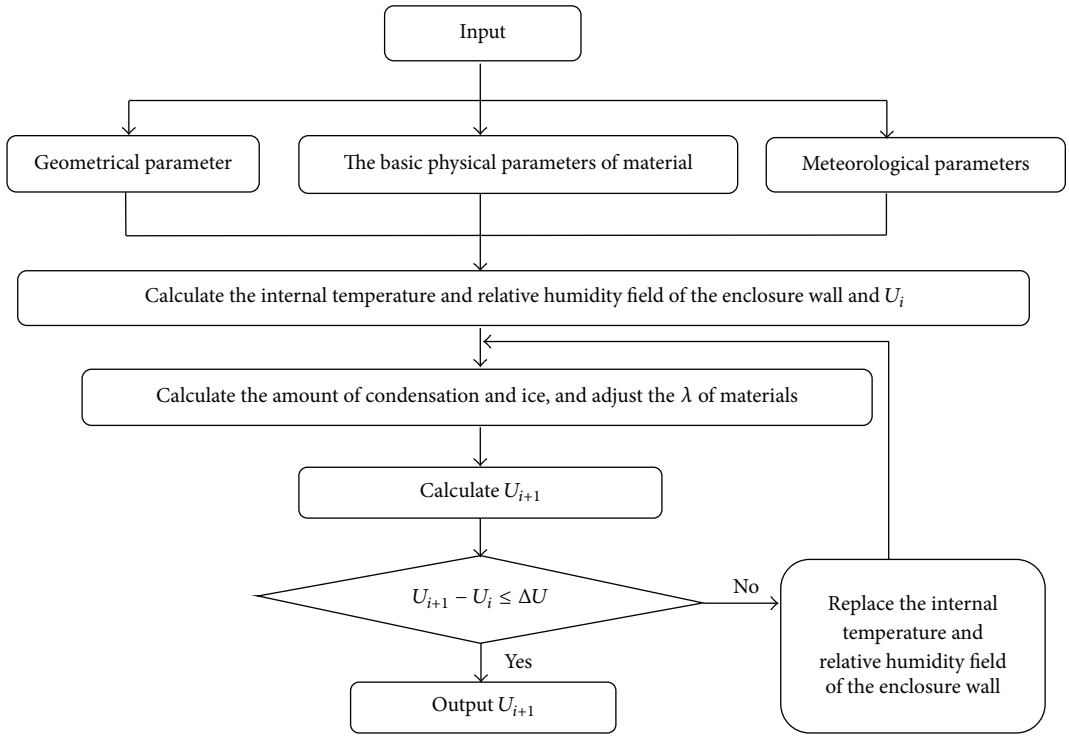

Figure 5: The process of calculating the corrected value of heat transfer coefficient.

Table 3: Comparison between experimental values and theoretical values of wall heat transfer coefficients.

Sample types	Experimental values (m^2 K W^{-1})	Theoretical values (m^2 K W^{-1})
SJ0	1.607 (1 ± 2.06%)	—
SJ1	2.046 (1 ± 2.04%)	—
SJ2	0.497 (1 ± 2.33%)	0.522
SJ3	0.391 (1 ± 2.20%)	0.519

of SJ1; experimental value of heat transfer coefficient of SJ2 was lower than that of SJ1; after adding 60 mm unilateral EPS template, the wall heat transfer coefficient of SJ2 was reduced by 76%, and the energy saving effects significantly increased. After adding 60 mm EPS template in the middle of recycled concrete bricks wall, the wall heat transfer coefficient of SJ3 was reduced by 81%; heat transfer coefficient value of SJ3 is less than that of SJ2.

The heat transfer coefficients of the samples are different between experimental values and theoretical values. Theoretical value using the boundary layer of thermal resistance and material coefficient of thermal conductivity are different from material coefficient of thermal conductivity corrected value. The error of the sample material size has large influence on heat transfer coefficient of the theoretical value calculated. U was strongly, significantly related to the thickness of EPS template (d) (Figure 6), decreasing with rising thickness of EPS template. The fitted lines in Figure 6 were derived from the empirical model ($U = 1/(a + x/b)$). Heat transfer

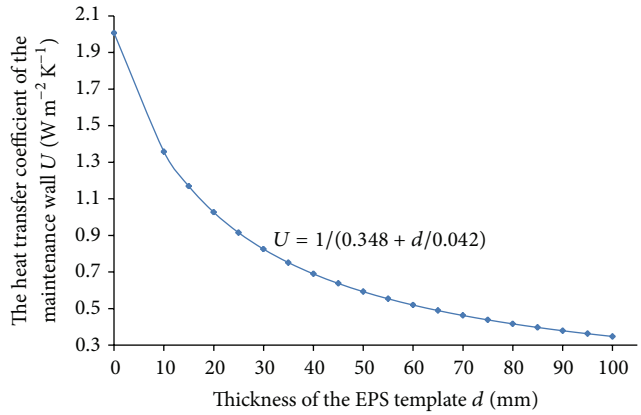

Figure 6: The relationship between the thickness of the EPS template and heat transfer coefficient.

coefficient values of the maintaining wall decreased with increasing thickness of the EPS insulation board (Figure 6). It showed that after adding thinner EPS insulation board, the heat transfer coefficient could be greatly reduced. However, with the constantly increasing thickness of EPS insulation board, heat transfer coefficient value are no longer significantly decreased. Similarly, the thermal resistance of sample has a monotone increasing ratio of the total thermal resistance, and the speed slows down. Through the calculation result, 60 mm EPS insulation board decreased the thickness of 5 mm, and the maintenance wall heat transfer coefficient increases by 6.6%.

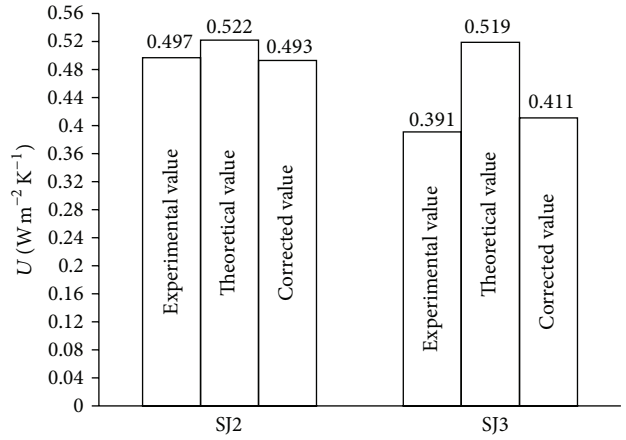

Figure 7: Comparison between experimental values, theoretical values, and corrected values of wall heat transfer coefficients.

4.4. Results Analysis of Correct Calculation of Heat Transfer Coefficient. According to the true value calculation model of heat transfer coefficient, heat transfer coefficients of SJ2 and SJ3 were evaluated in the test environment, and Figure 7 showed the results of the comparison between the theoretical values and experimental values.

Figure 7 showed the results; when considering the influences of temperature and humidity on materials change, the heat transfer coefficients of corrected calculation values were all lower than theoretical values and much closer to the experimental values, which could prove that corrected computation was correct and reflect the heat transfer performance accurately.

5. Conclusions

In this study, four tactic forms of wall samples were tested to investigate their heat transfer coefficients; the heat transfer coefficient of recycled concrete bricks wall is significantly reduced after obtaining composite EPS insulation board. The heat transfer coefficient of both sides of recycled concrete bricks wall with middle 60 mm EPS insulation board not only is less than the same thickness of the external insulation but also has excellent durability. Based on the basic mechanism of the thermal conductivity of recycled concrete bricks and EPS insulation board, the relationship between coefficient of thermal conductivity of various materials and temperature, humidity could be derived. According to expression of the true thermal conductivity of material, calculation methods of heat transfer coefficient of recycled concrete bricks composite EPS insulation board wall have been proposed. By analyzing the experimental values, the theoretical values, and the corrected values of the test samples, the corrected-value calculation method was proved to be correct and reasonable and can achieve better energy efficiency.

Conflict of Interests

The authors declare that there is no conflict of interests regarding the publication of this paper.

Acknowledgments

This research was supported by Beijing University of Technology and Grants from Natural Science Foundation of China (51308011) and National Science and Technology Support Project of China (2011BAJ08B02). The authors thank Beijing Building Materials Test Center for assistance with the testing instruments.

References

[1] B. Li and R. Yao, "Urbanisation and its impact on building energy consumption and efficiency in China," *Renewable Energy*, vol. 34, no. 9, pp. 1994–1998, 2009.

[2] C. Peng and Z. Wu, "In situ measuring and evaluating the thermal resistance of building construction," *Energy and Buildings*, vol. 40, no. 11, pp. 2076–2082, 2008.

[3] X. Xu and S. Wang, "Optimal simplified thermal models of building envelope based on frequency domain regression using genetic algorithm," *Energy and Buildings*, vol. 39, no. 5, pp. 525–536, 2007.

[4] L. D. D. Harvey, "Reducing energy use in the buildings sector: measures, costs, and examples," *Energy Efficiency*, vol. 2, no. 2, pp. 139–163, 2009.

[5] A. Seppälä, M. El Haj Assad, and T. Kapanen, "Optimal structure for heat and cold protection under transient heat conduction," *Structural and Multidisciplinary Optimization*, vol. 36, no. 4, pp. 355–363, 2008.

[6] C.-M. Lai and Y.-H. Wang, "Energy-saving potential of building envelope designs in residential houses in Taiwan," *Energies*, vol. 4, no. 11, pp. 2061–2076, 2011.

[7] Z. Ge, R. J. Sun, and Z. Li, "Mechanical properties of concrete with recycled clay-brick-powder," *Advanced Building Materials*, vol. 250–253, pp. 360–364, 2011.

[8] A. J. Lohonyai, Y. Korany, and M. D. Ross, "Effective foam insulation for single-wythe concrete masonry walls," *Journal of Building Physics*, vol. 37, no. 2, pp. 200–210, 2013.

[9] I. Marcelo, V. Maria, J. Daniel, and R. Pedro, "Life cycle and optimum thickness of thermal insulator for housing in madrid," in *The 2005 World Sustainable Building Conference*, pp. 418–425, In-house Publishing, Rotterdam, The Netherlands, 2005.

[10] T. Vrána and F. Björk, "A laboratory equipment for the study of moisture processes in thermal insulation materials when placed in a temperature field," *Construction and Building Materials*, vol. 22, no. 12, pp. 2335–2344, 2008.

[11] P. Zbysek and C. Robert, "Hygrothermal performance study of an innovative interior thermal insulation system," *Applied Thermal Engineering*, vol. 29, no. 10, pp. 1941–1946, 2009.

[12] C.-F. Liang, B.-X. Sun, Q. Liu, and W.-H. Bai, "Effect of air layer on coupled heat and moisture transfer in EPS external insulation walls," *Journal of Building Materials*, vol. 15, no. 6, pp. 803–808, 2012.

[13] Standardization Administration of the People's Republic of China, "Thermal insulation—determination of steady-state thermal transmission properties—calibrated and guard hot box," Tech. Rep. GB/T 13475-2008, China Standards Press, Beijing, China, 2008.

[14] ASTM C1363, *Standard Test Method for Thermal Performance of Building Materials and Envelope Assemblies by Means of a Hot Box Apparatus*, American Society for Testing and Materials, West Conshohocken, Pa, USA, 2005.

[15] ISO, "Thermal insulation-determination of steady-state thermal transmission properties-calibrated and guarded hot box," ISO 8990, International Organization for Standardization, 1994.

[16] "Assembly of Technical standard for building energy saving and innovation technology of wall materials in Beijing," in *The Office of Building Energy Saving and Wall Materials Innovation in Beijing*, pp. 34–39, Standards Press of China, Beijing, China, 1999.

[17] Q. G. Chen, *The Basis of Building Thermal Physical*, Xi'an Jiaotong University Press, Xi'an, China, 1991.

[18] Z. L. Chen and M. F. Tang, *Building Physics*, Building Industry Press of China, Beijing, China, 2009.

[19] M. Jerman and R. Černý, "Effect of moisture content on heat and moisture transport and storage properties of thermal insulation materials," *Energy and Buildings*, vol. 53, pp. 39–46, 2012.

[20] I. Gnip, S. Vejelis, and S. Vaitkus, "Thermal conductivity of expanded polystyrene (EPS) at 10°C and its conversion to temperatures within interval from 0 to 50°C," *Energy and Buildings*, vol. 52, pp. 107–111, 2012.

[21] *Guide to the Expression of the Uncertainty in Measurements*, International Organization for Standardization, (ISO), 1995.